

Hydrogenation of Synthetic *cis*-1,4-Polyisoprene and Natural Rubber Catalyzed by $[\text{Ir}(\text{COD})\text{py}(\text{PCy}_3)]\text{PF}_6$

Napida Hinchiranan,¹ Kitikorn Charmondusit,¹ Pattarapan Prasassarakich,¹ Garry L. Rempel²

¹Department of Chemical Technology, Faculty of Science, Chulalongkorn University, Bangkok 10330, Thailand

²Department of Chemical Engineering, University of Waterloo, Ontario, Canada N2L3G1

Received 7 February 2005; accepted 17 August 2005

DOI 10.1002/app.23710

Published online in Wiley InterScience (www.interscience.wiley.com).

ABSTRACT: In the presence of chlorinated solvents, the catalytic complex $[\text{Ir}(\text{COD})\text{py}(\text{PCy}_3)]\text{PF}_6$ (where COD is 1,5-cyclooctadiene and py is pyridine) was an active catalyst for the hydrogenation of synthetic *cis*-1,4-polyisoprene and natural rubber. Detailed kinetic and mechanistic studies for homogeneous hydrogenation were carried out through the monitoring of the amount of hydrogen consumed during the reaction. The final degree of olefin conversion, measured with a computer-controlled gas-uptake apparatus, was confirmed by Fourier transform infrared spectroscopy and ¹H-NMR spectroscopy. Synthetic *cis*-1,4-polyisoprene was used as a model polymer for natural rubber without impurities to study the influence of the catalyst loading, polymer concentration, hydrogen pressure, and reaction temperature with a statistical design framework. The kinetic results for the hydrogenation of both synthetic *cis*-1,4-polyisoprene and natural rubber indicated that the hydrogenation rate exhibited a first-order dependence on the catalyst concentration and hydrogen pressure. Because of impurities inside the natural

rubber, the hydrogenation of natural rubber showed an inverse behavior dependence on the rubber concentration, whereas the hydrogenation rate of synthetic rubber, that is, *cis*-1,4-polyisoprene, remained constant when the rubber concentration increased. The hydrogenation rate was also dependent on the reaction temperature. The apparent activation energies for the hydrogenation of synthetic *cis*-1,4-polyisoprene and natural rubber were evaluated to be 79.8 and 75.6 kJ/mol, respectively. The mechanistic aspects of these catalytic processes were discussed on the basis of observed kinetic results. The addition of some acids showed an effect on the hydrogenation rate of both rubbers. The thermal properties of hydrogenated rubber samples were determined and indicated that hydrogenation increased the thermal stability of the hydrogenated rubber but did not affect the inherent glass-transition temperature. © 2006 Wiley Periodicals, Inc. *J Appl Polym Sci* 100: 4219–4233, 2006

Key words: catalysts; modification; rubber

INTRODUCTION

Natural rubber (NR) harvested from *Hevea Brasiliensis* has been used in many applications because of its excellent properties, including superior building tack, green stock strength, better processing, high strength in nonblack formulations, hot tear resistance, retention of strength at elevated temperatures, high resilience, low heat buildup, and general fatigue resistance.¹ NR is predominantly composed of the isoprene unit in a *cis*-1,4 configuration. The remarkable difference between NR and synthetic *cis*-1,4-polyisoprene (CPIP) is the presence of nonrubber components such as proteins in NR, which are believed to bring about its characteristic properties.² Because of the unsaturation of the isoprene backbone, NR deteriorates in the presence of oxygen, ozone, sunlight, and long-term heat-

ing. Chemical modification of polymers is a postpolymerization process used to produce polymers with desirable properties that are not accessible by general polymerization.³ Hydrogenation, one form of chemical modification, has been used to reduce the saturation of diene polymers to enhance the thermal and oxidative resistance of the polymers. Usually, hydrogenation can be provided by catalytic or noncatalytic methods. The noncatalytic technique uses a hydrogenation reagent, such as a diimide generated in situ from *p*-toluenesulfonylhydrazide (TSH).⁴ Nevertheless, the reaction of polyisoprene with TSH at 140°C could only produce a low level of hydrogenation (<40% conversion), despite the use of a large amount of TSH. In addition, the polymer was partially depolymerized and cyclized.

Because of disadvantages of the noncatalytic method, catalytic hydrogenation has been increasingly studied. Heterogeneous catalysts such as Pd/Al₂O₃, Pd/CaCO₃, and Pd/BaSO₄ can be used as catalysts for the hydrogenation of polymers.^{5,6} Although heterogeneous catalysts do not have the problem of residue-metal removal, a mass-transfer limitation is the main disadvantage in limiting their catalytic activity. Thus,

Correspondence to: G. L. Rempel (grempe@cape.uwaterloo.ca).

Contract grant sponsor: Thailand Research Fund (through the Royal Golden Jubilee Project).

Contract grant sponsor: Natural Sciences and Engineering Research Council of Canada.

the process requires the use of a high catalyst concentration and a long reaction time to obtain the desired level of hydrogenation.

Homogeneous catalysts are favorable as catalysts for the hydrogenation of unsaturated polymers with or without sensitive functional groups such as —CN or CO_2H because of their higher selectivity and absence of macroscopic diffusion problems.⁷ Homogeneous catalysts for the hydrogenation of diene-based polymers have generally been dominated by complexes of group VIII transition metals in the second row of the periodic table, such as rhodium, ruthenium, and palladium complexes.

For the potential of transition metals in the third row, it has previously been thought that they have less catalytic activity than those of the second row. However, iridium-based catalysts have been shown to be efficient catalysts for hydrogenation.⁸ The judicious choices of a suitable metal–ligand system, solvent, and reaction conditions may lead to highly efficient catalysts.

An analogue of the $[\text{MCl}(\text{PPh}_3)_3]$ complexes, the rhodium complex called Wilkinson's catalyst is one of the most efficient catalysts for the hydrogenation of unsaturated substrates, whereas cobalt and iridium analogues are totally inactive. The cobalt complex fails to react with hydrogen, but the iridium analogue reacts irreversibly with hydrogen to give a stable adduct $[\text{IrClH}_2(\text{PPh}_3)_3]$, which fails to dissociate PPh_3 to allow the substrate access to the active site.⁸ Crabtree et al.⁹ discovered that the use of chlorinated solvents such as CHCl_3 , $\text{C}_6\text{H}_5\text{Cl}$, and CH_2Cl_2 enhanced the catalytic activity of iridium catalysts, whereas $[\text{Ir}(\text{COD})\text{L}_2]\text{PF}_6$ and $[\text{Ir}(\text{COD})\text{L}(\text{py})]\text{PF}_6$ (where COD is 1,5-cyclooctadiene, py is pyridine, and L is tertiary phosphine) in solvents such as benzene, toluene, and hexane were disappointing in promoting the activity of the iridium catalyst because only catalytically inactive precipitates were formed under hydrogen. The chlorinated solvents are the only viable solvents for catalytic hydrogenation with these cationic iridium catalysts, presumably because they have high polarity but negligible coordinating power.⁸ They found that these iridium catalysts showed much smaller rate differences between monosubstituted, disubstituted, trisubstituted, and tetrasubstituted alkenes. Another advantage of these iridium catalysts is that both the precursors and the catalyst themselves are stable to other oxidizing reagents, such as O_2 or EtI , which generally rapidly deactivate other hydrogenation catalysts.

There are some previous research reports on the hydrogenation of diene-based polymers catalyzed by iridium catalysts. Gilliom and a coworker^{10,11} studied the catalytic hydrogenation of polybutadiene and a butadiene–styrene triblock copolymer with $[\text{Ir}(\text{COD})(\text{PMePh}_2)_2]\text{PF}_6$ as a catalyst in the absence of a solvent under moderate conditions. Hu¹² studied the kinetics of the hydrogenation of nitrile–butadiene rubber with $[\text{Ir}(\text{COD})\text{py}(\text{PCy}_3)]\text{PF}_6$.

In this study, the objective of the research was to study and compare the hydrogenation of synthetic CPIP and that of NR catalyzed by $[\text{Ir}(\text{COD})\text{py}(\text{PCy}_3)]\text{PF}_6$ and to investigate the effect of the reaction parameters on the hydrogenation rate, such as the catalyst concentration, rubber concentration, hydrogen pressure (P_{H_2}), and reaction temperature. The kinetics of the reaction and a proposed mechanism for CPIP and NR hydrogenation by $[\text{Ir}(\text{COD})\text{py}(\text{PCy}_3)]\text{PF}_6$ are reported. The effect of the addition of some acids on the hydrogenation rate and the thermal properties of the hydrogenated rubbers were also investigated.

EXPERIMENTAL

Materials

High-molecular-weight CPIP with 97% cis isomer (Natsyn) was provided by Bayer, Inc. (Sania, Canada). Solid NR (STR-5L) was obtained from Chalong Latex Industry Co., Ltd. (Songkhla, Thailand). Crabtree's catalyst, $[\text{Ir}(\text{COD})\text{py}(\text{PCy}_3)]\text{PF}_6$, was purchased from Strem Chemicals (Newburyport, MA) or synthesized as described in the literature,¹³ Reagent-grade toluene was obtained from BDH Chemicals (Toronto, Canada). Chlorobenzene, tetrahydrofuran, dichloromethane, and chloromethane were purchased from Fisher Scientific, Ltd. (Fairlawn, NJ). Ethanol, 3-chloropropionic acid (3-CPA), and *p*-toluenesulfonic acid (*p*-TSA) were obtained from Aldrich Chemical Co., Inc. (Milwaukee, WI). All solvents were used as received. The reaction gas used in the hydrogenation was oxygen-free hydrogen with a purity of 99.99% obtained from Praxair, Inc. (Kitchener, Canada).

Kinetic study of hydrogenation

Kinetic data provided from hydrogen consumption profiles were obtained with the gas-uptake apparatus developed by Mohammadi and Rempel.¹⁴ This equipment can maintain isothermal ($\pm 1^\circ\text{C}$) and isobaric (± 0.02 bar) conditions. The hydrogenation of CPIP and NR was started with the preparation of the rubber solution through the dissolution of the desired amount of the rubber in 150 mL of monochlorobenzene in the dark. The catalyst powder, $[\text{Ir}(\text{COD})\text{py}(\text{PCy}_3)]\text{PF}_6$, was weighted in a small glass bucket and placed in a port of the reactor head. The rubber solution was degassed via charging with hydrogen gas at 13.8 bar three times, followed by the continuous bubbling of hydrogen gas through the solution for 20 min at a 1200 rpm agitation speed to ensure that oxygen was completely removed from the system. Once the experimental equilibrium temperature and pressure were established, the powder complex of $[\text{Ir}(\text{COD})\text{py}(\text{PCy}_3)]\text{PF}_6$ was dispersed in the solution

with a slight overpressure of hydrogen. The amount of hydrogen consumed by the reaction and the reaction temperature were then recorded as a function of time. Each experiment proceeded until gas consumption ceased, after which the reactor was quickly cooled and the product was isolated by precipitation with ethanol, followed by drying in vacuo.

Characterization

The structure of hydrogenated rubbers and the exact final degree of olefin conversion provided by the hydrogen consumption profile were investigated with Fourier transform infrared (FTIR) spectroscopy and $^1\text{H-NMR}$ spectroscopy. FTIR spectra were obtained with a Bio-Rad FTS 3000X spectrometer. The infrared samples were prepared via the casting of polymer films from solution onto a sodium chloride disk in an oven maintained at 70°C . $^1\text{H-NMR}$ spectra of the polymer samples were recorded on a Bruker 300-MHz spectrometer, with CDCl_3 as the solvent.

Viscosity measurements

The relative viscosity (η_{rel}) of dilute polymer solutions (0.12500 ± 0.00015 g of hydrogenated rubber in 25 mL of toluene) was measured at 35°C with an Ubbelohde capillary viscometer. The samples were filtered through a coarse, sintered-glass filter to separate the insoluble gel in the rubber solutions. The η_{rel} data were reported as the viscosity with respect to the pure solvent.

Thermogravimetric analysis (TGA)

TGA of the samples of synthetic CPIP before and after hydrogenation was carried out on a Netzsch STA 409C (Schwerzendenbach, Switzerland), and TGA of NR and its hydrogenated product was performed on a Pyris Diamond thermogravimetric/differential thermal analysis instrument (Tokyo, Japan). The rubber sample was placed in an aluminum crucible. The temperature was raised under a nitrogen atmosphere from room temperature to 700°C at a constant heating rate of $10^\circ\text{C}/\text{min}$. The nitrogen gas flow rate was $50\text{ mL}/\text{min}$. The initial decomposition temperature (T_{id}) and the temperature at the maximum mass-loss rate (T_{max}) were evaluated.

Differential scanning calorimetry (DSC)

DSC of a sample of synthetic CPIP before and after hydrogenation was conducted with a Netzsch DSC 200 (Schwerzendenbach, Switzerland) with constant heating rate of $10^\circ\text{C}/\text{min}$, and DSC of NR and its hydrogenated product was performed on a Mettler-Toledo DSC 822 with a constant heating rate of $20^\circ\text{C}/\text{min}$. For heat-flux DSC, the instrument signal was derived from the temperature difference between the

sample and the reference. The equipment was calibrated with indium. The rubber sample in a crimped aluminum pan was first cooled in a cell to -100°C with liquid nitrogen and then heated up to over 0°C . The midpoint of the baseline shift was taken as the glass-transition temperature (T_g).

RESULTS AND DISCUSSION

Characterization of hydrogenated *cis*-1,4-polyisoprene (HCPIP) and hydrogenated natural rubber (HNR)

The structure of synthetic CPIP and NR before and after the hydrogenation process was preliminarily characterized with FTIR spectroscopy, as shown in Figure 1. The structures of both hydrogenated rubbers are similar to an alternating ethylene-propylene copolymer (EPDM). The characteristic FTIR peaks of both hydrogenated rubbers show that the absorption bands corresponding to the $\text{C}=\text{C}$ stretching, olefinic $\text{C}-\text{H}$ bending, and $-(\text{CH}_2)_3-$ are located at 1664, 836, and 743 cm^{-1} , respectively. The characteristic signals of unsaturation, 1664 and 836 cm^{-1} , disappeared in the hydrogenated rubbers, whereas an intense signal appeared at 739 cm^{-1} due to saturated carbon formed through hydrogenation. For the FTIR spectrum of NR, the weak transmittance bands at 3285 ($>\text{N}-\text{H}$) and 1531 cm^{-1} ($>\text{N}-\text{C}=\text{O}$)¹⁵ remained constant after hydrogenation.

$^1\text{H-NMR}$ spectroscopy was used to investigate the actual degree of hydrogenation in each sample. The $^1\text{H-NMR}$ spectra of CPIP and NR before and after the hydrogenation reaction are shown in Figure 2. There is a sizeable reduction in the olefinic proton signal at 5.1 ppm, which confirms that the carbon-carbon double bond in CPIP and NR was hydrogenated. The aliphatic proton signals at 0.8 and 1.2 ppm, attributed to saturated $-\text{CH}_3$ and $-\text{CH}_2-$ groups, show a strong increment due to the chemical transformation of double bonds upon saturation. The actual degree of hydrogenation could be calculated from the peak area at 5.1 ppm and the summation of the peak area between 0.8 and 2.0 ppm.

Kinetic experiments of synthetic CPIP and NR hydrogenation

All the kinetic data for CPIP and NR hydrogenation in the presence of the homogeneous catalyst, $[\text{Ir}(\text{COD})\text{-py}(\text{PCy}_3)]\text{PF}_6$, were obtained with the gas-uptake apparatus. The kinetic experiments were conducted with a factorial design of experiments to find the main and interaction effects of the system and with univariate experiments to investigate the effect of each factor individually. The rate of reaction in the entire system, based on an overall second-order reaction, could be expressed as follows:

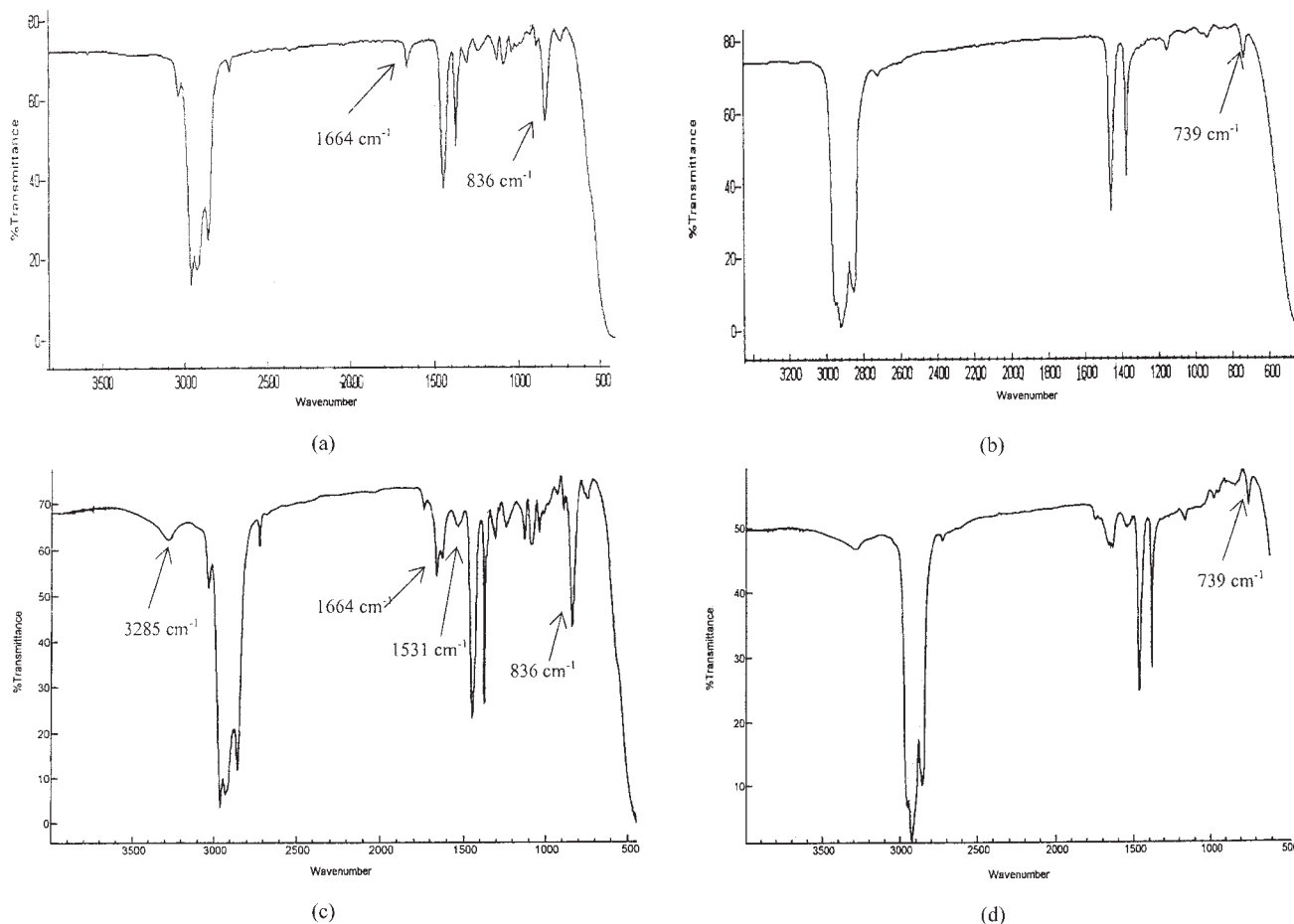


Figure 1 FTIR spectra of (a) CPIP, (b) HCIPL, (c) NR, and (d) HNR.

$$-\frac{d[\text{C}=\text{C}]}{dt} = k[\text{C}=\text{C}][\text{H}_2] \quad (1)$$

where k is the reaction rate constant and $[\text{C}=\text{C}]$ and $[\text{H}_2]$ are the concentrations of unsaturated double bonds and dissolved hydrogen in the solvent, respectively. All kinetic data were collected with a constant, high P_{H_2} value, with vigorous mixing. Therefore, $[\text{H}_2]$ was assumed to be in equilibrium with the gaseous pressure and remained constant during the course of reaction. Consequently, the reaction could be approximated as a pseudo-first-order reaction:

$$-\frac{d[\text{C}=\text{C}]}{dt} = k'[\text{C}=\text{C}] \quad (2)$$

where k' is the pseudo-first-order rate constant. Figure 3(a-1,b-1) shows representative plots of the conversion versus time for the hydrogenation reactions of CPIP and NR, respectively. The hydrogen consumption plot indicates that the reaction was apparently first-order in the olefinic substrate, according to eq. (1). Equation (3) is further expressed in terms of the conversion of

unsaturated double bonds (x ; i.e., the extent of hydrogenation) as follows:

$$\ln(1 - x) = -k't \quad (3)$$

where t is the reaction time. Figure 3(a-2,b-2) shows a linear plot of $\ln(1 - x)$ versus time for CPIP and NR hydrogenation. The pseudo-first-order rate constant was then readily determined from the slope of the corresponding curve. The difference between the natural logarithm plot of CPIP hydrogenation and that of NR hydrogenation was that the initial phase of NR hydrogenation was slower. Presumably, the catalyst required some time to be dissolved in the NR solution, and some impurities in NR might have retarded the rate of reaction in the initial period.

Experimental design

The principle of a kinetic study is to investigate the relationship between the reaction rate and the condition under which the reaction is carried out. The rate of CPIP and NR hydrogenation is known to be

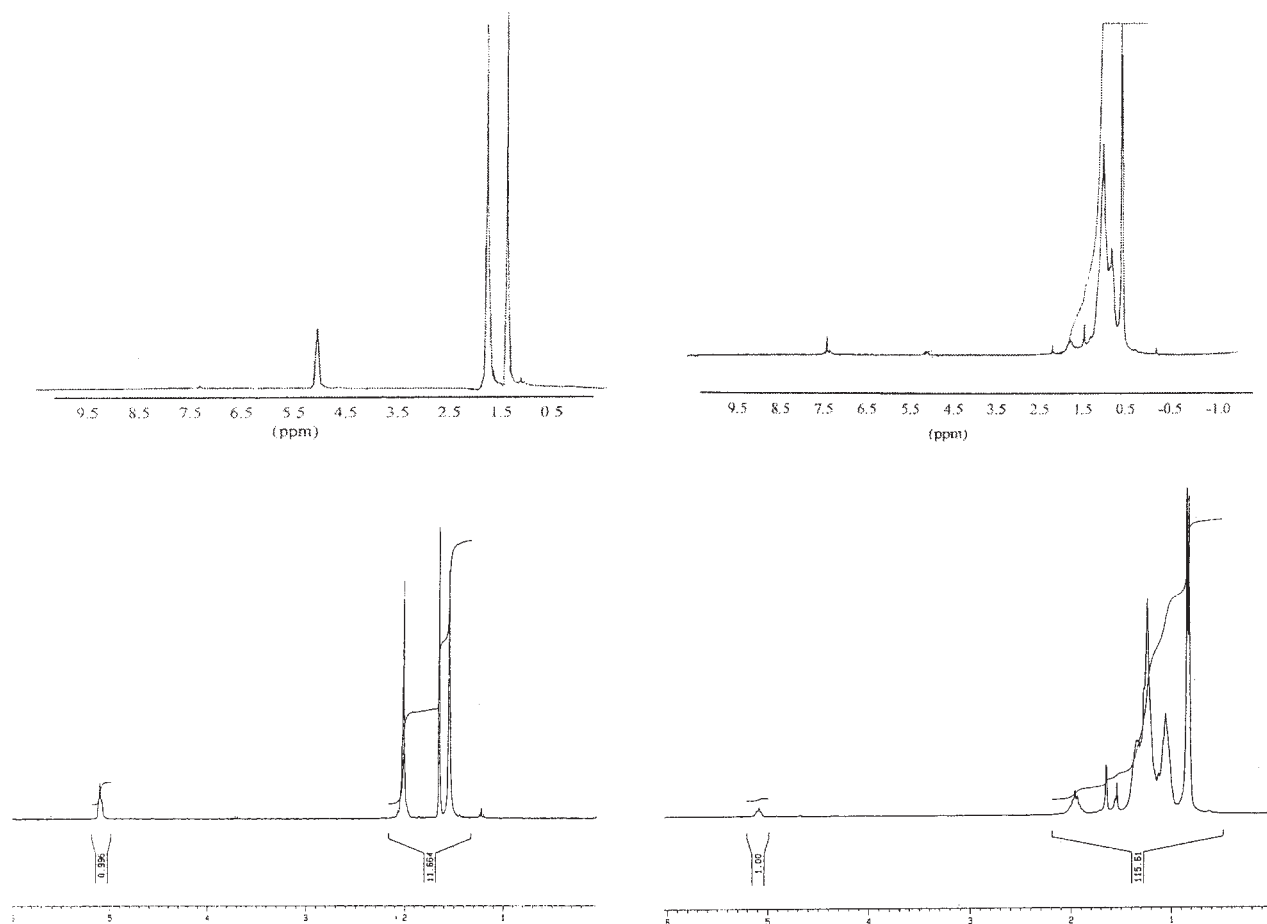


Figure 2 $^1\text{H-NMR}$ spectra of (a) CPIP, (b) HCPIP, (c) NR, and (d) HNR.

influenced by factors such as the concentrations of the catalyst ($[\text{Ir}]$) and rubber ($[\text{C}=\text{C}]$) and P_{H_2} as well as the reaction temperature. Experimental conditions were assigned according to a central composite structure¹⁶ composed of a two-level factorial design and a series of univariate experiments. The first component consisted of a 2^3 factorial design of the principal factors of interest ($[\text{Ir}]$, $[\text{C}=\text{C}]$, and P_{H_2}) that had an effect on k' and the catalytic cycle of $[\text{Ir}(\text{COD})\text{py}(\text{PCy}_3)]\text{PF}_6$. The univariate or one-at-a-time experiments with respect to $[\text{Ir}]$, $[\text{C}=\text{C}]$, P_{H_2} , and temperature examined the influence of each factor acting alone. By varying a single factor in isolation, these studies defined the relationship between the catalyst activity and the process factor in greater detail. The selection of an appropriate range for each factor considered the catalyst weighing precision, the polymer solution viscosity, and the reaction rate that the apparatus could control and monitor effectively.

Two-level factorial design experiment

In this work, the hydrogenation of CPIP in the presence of $[\text{Ir}(\text{COD})\text{py}(\text{PCy}_3)]\text{PF}_6$ was used as a prelim-

inary study to investigate the main effects and joint effects of reaction parameters. The response for each variable was the rate constant. The levels of the factors were arbitrarily called low (-) and high (+). The ranges of $[\text{Ir}]$, $[\text{C}=\text{C}]$, and P_{H_2} were 80–100 μM , 246 to 500 mM, and 20.7 to 34.5 bar, respectively, in monochlorobenzene at a constant reaction temperature of 130°C. The results of the factorial experiment are summarized in Table I. Yates's algorithm was applied to calculate the main effects and interaction effects on the rate constant derived from the experimental data. The Yates calculation for the hydrogenation of CPIP and the results of the factorial design analysis are shown in Tables II and III, respectively. The results in Table III indicate that $[\text{Ir}]$ and P_{H_2} had a positive influence on the rate of hydrogenation, whereas $[\text{C}=\text{C}]$ exhibited a negative result, which may be attributed to some impurities such as residual catalyst in the polymerization step, which may reduce the catalytic efficiency of the hydrogenation process. The binary interactions, $[\text{Ir}] \times P_{\text{H}_2}$, $[\text{Ir}] \times [\text{C}=\text{C}]$, and $P_{\text{H}_2} \times [\text{C}=\text{C}]$, and the three-factor interaction, $[\text{Ir}] \times P_{\text{H}_2} \times [\text{C}=\text{C}]$, were not highly significant.

TABLE I
Results from the 2^3 Factorial Design for CPIP
Hydrogenation at 130°C

Experiment	[Ir] (μM)	[C=C] (mM)	P_{H_2} (bar)	Temperature (°C)	$k' \times 10^3$ (s^{-1})
1	0.0796	246.08	20.7	130	1.26
2	0.0798	246.88	20.7	130	1.28
3	0.0997	246.37	20.7	130	1.41
4	0.0994	246.15	20.7	130	1.37
5	0.0801	246.57	34.5	130	2.41
6	0.0799	246.45	34.5	130	2.30
7	0.0996	245.88	34.5	130	2.68
8	0.0994	246.08	34.5	130	2.55
9	0.0801	500.19	20.7	130	0.89
10	0.0800	500.04	20.7	130	0.91
11	0.1004	500.49	20.7	130	1.35
12	0.0994	500.39	20.7	130	1.42
13	0.0797	500.58	34.5	130	2.04
14	0.0798	500.19	34.5	130	2.16
15	0.1001	500.49	34.5	130	2.20
16	0.1003	500.29	34.5	130	2.35

Univariate kinetic experiments

Although the results of the 2^3 factorial design are unable to explore fully a wide region in the factor space, they can indicate major trends and help to determine a promising direction for further experimentation. The univariate components of the central composite design augment the factorial study by exploring how each factor influences the hydrogenation rate in isolation. The experimental factors are varied one at a time, with the remaining factors held constant. This method provides an estimation of the effect of a single variable at selected fixed conditions of the other variables. In this section, the results from univariate experiments of CPIP hydrogenation are compared with those of the NR hydrogenation. The results of these experiments are summarized in Tables IV and V. The compared kinetic data of hydrogenation for both rubbers are presented in Figures 4–7.

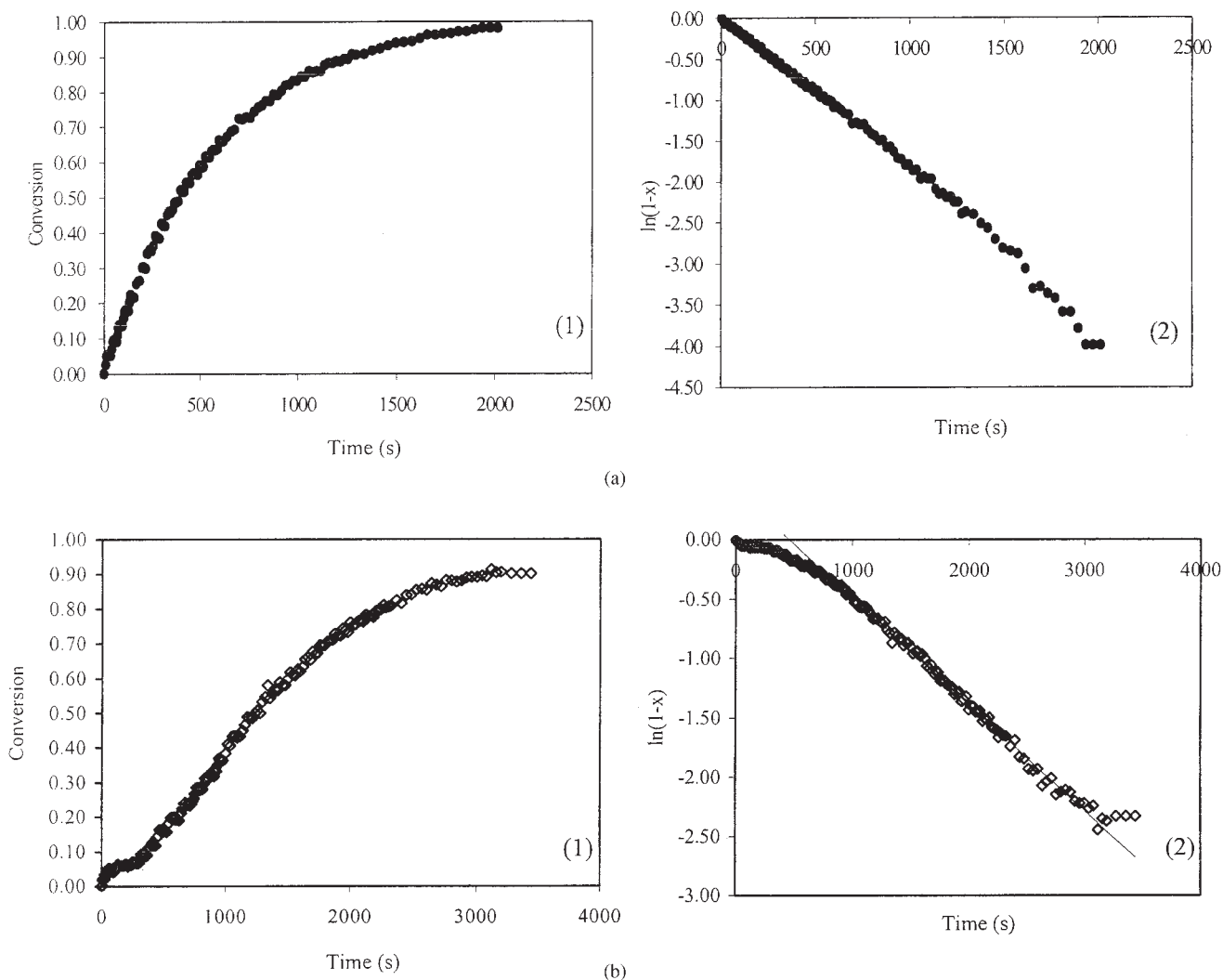


Figure 3 (1) Olefin conversion profile and (2) first-order plot for (a) CPIP hydrogenation ($[\text{Ir}] = 90 \mu\text{M}$; $P_{\text{H}_2} = 27.6 \text{ bar}$; $[\text{C}=\text{C}] = 246 \text{ mM}$; temperature = 130°C) and (b) NR hydrogenation ($[\text{Ir}] = 105 \mu\text{M}$; $P_{\text{H}_2} = 27.6 \text{ bar}$; $[\text{C}=\text{C}] = 152 \text{ mM}$; temperature = 140°C).

TABLE II
Yates's Algorithm Calculation of the 2³ Factorial Experiments for CPIP Hydrogenation

Test	Design matrix variable			<i>k'</i> average (s ⁻¹)	Algorithm					
	[Ir]	<i>P</i> _{H₂}	[C=C]		1	2	3	Divisor	Estimate	Identification
1	-	-	-	0.00127	0.00266	0.00764	0.01431	8	0.00179	Average
2	+	-	-	0.00139	0.00498	0.00667	0.00105	4	0.00026	[Ir]
3	-	+	-	0.00236	0.00229	0.00038	0.00440	4	0.00110	<i>P</i> _{H₂}
4	+	+	-	0.00262	0.00438	0.00067	-0.00017	4	-0.00004	[Ir] × <i>P</i> _{H₂}
5	-	-	+	0.00090	0.00012	0.00232	-0.00097	4	-0.00024	[C=C]
6	+	-	+	0.00139	0.00026	0.00209	0.00029	4	0.00007	[Ir] × [C=C]
7	-	+	+	0.00210	0.00049	0.00014	-0.00023	4	-0.00006	<i>P</i> _{H₂} × [C=C]
8	+	+	+	0.00228	0.00018	-0.00031	-0.00045	4	-0.00011	[Ir] × <i>P</i> _{H₂} × [C=C]

[Ir] = (-) 80 or (+) 100 μM;
*P*_{H₂} = (-) 20.7 or (+) 34.5 bar;
[C=C] = (-) 246 or (+) 500 mM.

Effect of the catalyst concentration. The effect of the catalyst concentration for CPIP and NR hydrogenation was investigated through the variation of the catalyst concentrations, as shown in Figure 4. The range of catalyst loadings for the hydrogenation of CPIP (246 mM) was 30–150 μM at 130°C, and the range of catalyst concentrations for the hydrogenation of NR (152 mM) was 50–165 μM at 140°C. *P*_{H₂} was constant at 27.6 bar in chlorobenzene for all experiments. The results suggest that a first-order dependence on the catalyst concentration occurred below about 100 μM for CPIP hydrogenation. The higher load of the catalyst caused a zero-order dependence on the catalyst concentration. A well-known side reaction, the dimerization of the coordinatively unsaturated catalytically active species to inactive complexes such as [H₂Ir₂(μ-H)₃(PCy₃)₄]PF₆, might be employed to interpret this phenomenon.¹⁷ The hydrogenation exhibited a first-order dependence on the catalyst precursor loading, which implied that the active complex was a mononuclear species. Figure 4 also shows a comparison of the catalytic activity of the Ir complex for CPIP and

NR hydrogenation. The observation indicated that the NR hydrogenation required the use of a higher loading of the catalyst, although the rubber concentration of NR (152 mM) was less than that of CPIP (246 mM). It can be presumed that impurities in NR might reduce the catalytic activity; thus, some portion of the catalyst (ca. 50 μM) might be sacrificed because of a reaction with the impurities.

*Effect of *P*_{H₂}.* The effect of *P*_{H₂} on the hydrogenation rate was different in each catalyst system. The order of hydrogenation of acrylonitrile–butadiene rubber (NBR) in the presence of RhCl(PPh₃) with respect to *P*_{H₂} exhibited a first-to-zero-order dependence as the system pressure increased,¹⁸ whereas a second-to-zero-order behavior in *P*_{H₂} was found in the system catalyzed by OsHCl(CO)(O₂)(PCy₃)₂.^{19,20} To investigate the dependence of the hydrogenation rate on *P*_{H₂} for

TABLE IV
Kinetic Results of Univariate Experiments for CPIP Hydrogenation

Experiment	[Ir] (μM)	[C=C] (mM)	<i>P</i> _{H₂} (bar)	Temperature (°C)	<i>k'</i> × 10 ³ (s ⁻¹)
1	30.4	246.08	27.6	130	0.89
2	60.0	246.47	27.6	130	1.55
3	90.0	246.27	27.6	130	1.92
4	120.3	246.57	27.6	130	2.05
5	150.3	246.47	27.6	130	2.15
6	90.0	246.37	13.8	130	0.84
7	89.8	246.57	41.4	130	3.04
8	90.1	246.27	55.2	130	4.12
9	90.2	163.72	27.6	130	2.08
10	90.1	330.00	27.6	130	2.12
11	89.8	415.09	27.6	130	1.87
12	90.0	500.78	27.6	130	1.95
13	89.8	246.66	27.6	120	1.14
14	89.8	246.37	27.6	125	1.71
15	89.9	246.27	27.6	135	2.96
16	89.9	246.37	27.6	140	3.80

TABLE III
Calculated Effects and Standard Errors for the 2³ Factorial Experiments CPIP Hydrogenation

Effect	Estimate ± standard error
Average	0.00179 ± 1.69 × 10 ⁻⁵
Main effect	
[Ir]	0.00026 ± 3.38 × 10 ⁻⁵
<i>P</i> _{H₂}	0.00110 ± 3.38 × 10 ⁻⁵
[C=C]	-0.00024 ± 3.38 × 10 ⁻⁵
Two-factor interaction	
[Ir] × <i>P</i> _{H₂}	-0.00004 ± 3.38 × 10 ⁻⁵
[Ir] × [C=C]	0.00007 ± 3.38 × 10 ⁻⁵
<i>P</i> _{H₂} × [C=C]	-0.00006 ± 3.38 × 10 ⁻⁵
Three-factor interaction	
[Ir] × <i>P</i> _{H₂} × [C=C]	-0.00011 ± 3.38 × 10 ⁻⁵

TABLE V
Kinetic Results of Univariate Experiments
for NR Hydrogenation

Experiment	[Ir] (μM)	[C=C] (mM)	P_{H_2} (bar)	Temperature ($^{\circ}\text{C}$)	$k \times 10^3$ (s^{-1})
1	50	152.04	27.6	140	0.12
2	65	151.96	27.6	140	0.39
3	85	151.94	27.8	140	0.64
4	105	151.94	27.8	140	0.90
5	105	152.01	27.6	140	0.85
6	125	151.92	27.7	140	1.02
7	125	151.97	27.9	140	1.13
8	145	152.01	27.6	140	1.36
9	165	151.96	27.6	140	1.39
10	105	151.98	7.0	140	0.24
11	105	151.99	14.0	140	0.46
12	105	151.88	41.4	140	1.15
13	105	151.88	55.1	140	1.43
14	105	152.02	69.2	140	1.66
15	105	100.10	27.8	140	1.58
16	105	200.03	27.6	140	0.57
17	105	259.76	27.6	140	0.43
18	105	300.02	27.8	140	0.15
19	105	151.99	27.6	130	0.58
20	105	151.98	27.6	135	0.80
21	105	151.94	27.6	145	1.13
22	105	151.96	27.4	150	1.91

the hydrogenation of CPIP and NR, a series of experiments were carried out from 13.8 to 55.2 bar ($[\text{Ir}] = 90 \mu\text{M}$ and $[\text{C}=\text{C}] = 246 \text{ mM}$ at 130°C in monochlorobenzene) for CPIP hydrogenation and from 7.0 to 69.2 bar ($[\text{Ir}] = 105 \mu\text{M}$ and $[\text{C}=\text{C}] = 152 \text{ mM}$ at 140°C in monochlorobenzene) for NR hydrogenation. Plots of the rate constant versus P_{H_2} for both rubbers are fairly linear, as shown in Figure 5. This demonstrates that the rate of hydrogenation was first-order with respect

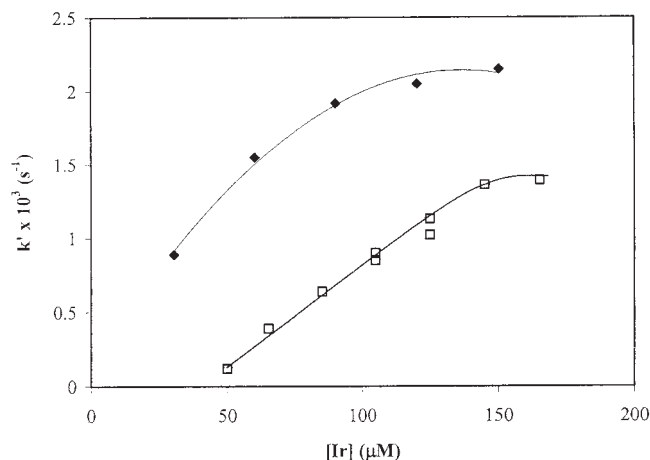


Figure 4 Effect of the catalyst concentration on the hydrogenation rate for (\blacklozenge) CPIP hydrogenation ($P_{\text{H}_2} = 27.6 \text{ bar}$; $[\text{C}=\text{C}] = 246 \text{ mM}$; temperature = 130°C) and (\square) NR hydrogenation ($P_{\text{H}_2} = 27.6 \text{ bar}$; $[\text{C}=\text{C}] = 152 \text{ mM}$; temperature = 140°C).

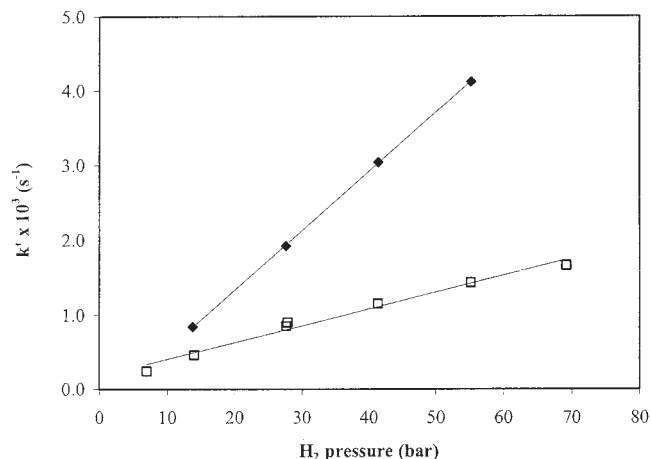


Figure 5 Effect of P_{H_2} on the hydrogenation rate for (\blacklozenge) CPIP hydrogenation ($[\text{Ir}] = 90 \mu\text{M}$; $[\text{C}=\text{C}] = 246 \text{ mM}$; temperature = 130°C) and (\square) NR hydrogenation ($[\text{Ir}] = 105 \mu\text{M}$; $[\text{C}=\text{C}] = 152 \text{ mM}$; temperature = 140°C).

to P_{H_2} . The first-order rate dependence implies that primarily a single reaction pathway was probably involved in the reaction of the unsaturation of the polymer with hydrogen. If more than one process were involved, the relative contribution of each pathway should have changed with varying P_{H_2} , and thus the dependence might deviate from first-order behavior. A first-order rate dependence on P_{H_2} was also observed in the hydrogenation of NBR with this iridium complex.¹²

Effect of the [C=C] concentration. The influence of the rubber concentration on the hydrogenation rate was studied over the range of 163–500 mM ($[\text{Ir}] = 90 \mu\text{M}$ and $P_{\text{H}_2} = 27.6 \text{ bar}$ at 130°C in monochlorobenzene) for CPIP hydrogenation and 100–300 mM ($[\text{Ir}] = 105$

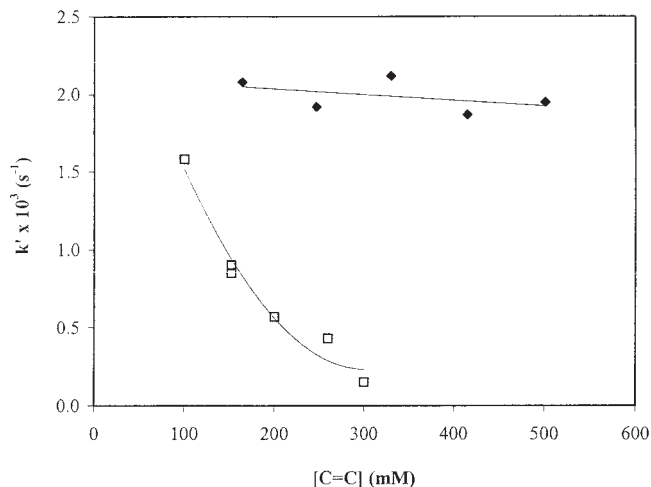


Figure 6 Effect of the C=C concentration on the hydrogenation rate for (\blacklozenge) CPIP hydrogenation ($[\text{Ir}] = 90 \mu\text{M}$; $P_{\text{H}_2} = 27.6 \text{ bar}$; temperature = 130°C) and (\square) NR hydrogenation ($[\text{Ir}] = 105 \mu\text{M}$; $P_{\text{H}_2} = 27.6 \text{ bar}$; temperature = 140°C).

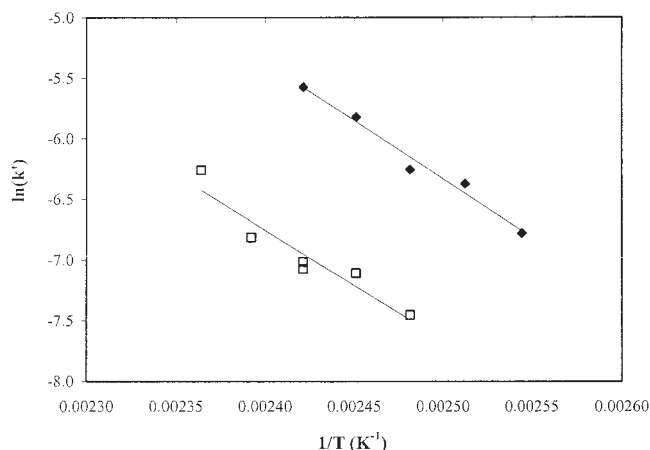


Figure 7 Arrhenius plot of (◆) CPIP hydrogenation ([Ir] = 90 μ M; P_{H_2} = 27.6 bar; [C=C] = 246 mM; temperature = 120–140°C) and (□) NR hydrogenation ([Ir] = 105 μ M; P_{H_2} = 27.6 bar; [C=C] = 152 mM; temperature = 130–150°C).

μ M and P_{H_2} = 27.6 bar at 140°C in monochlorobenzene) for NR hydrogenation. The results for the comparison are shown in Figure 6. The hydrogenation activity was essentially unaffected by the amount of CPIP. The conversion profiles for CPIP hydrogenation, which was first-order with respect to [C=C], were, by definition, independent of the amount of olefin charged to the reactor. This agrees with the observations of CPIP and styrene–butadiene copolymer hydrogenation with the osmium system, in which the C=C concentration had no effect on the hydrogenation rate.^{19,20} Unlike the case of CPIP hydrogenation, the relationship between the apparent rate constant and rubber concentration in NR hydrogenation illustrated that the reaction rate exhibited an inverse behavior with an increase in the loading of rubber. Crabtree et al.⁹ reported that iridium complexes [Ir(COD)(py)L]PF₆ and [Ir(COD)L₂]PF₆ were sensitive to a number of functional groups such as amines, which totally deactivate the catalysts by deprotonation. Accordingly, because proteins contributed a major impurity in NR, the catalytic activity of [Ir(COD)(py)(PCy₃)]PF₆ might be reduced by the amine contained in the protein structure. The influence of impurities in NR drastically decreased the efficiency of the Ir complex; thus, it was necessary to reduce the amount of NR or increase the reaction temperature to obtain a suitable reaction rate for the kinetic study. The effect of the rubber concentration on the hydrogenation rate of NR hydrogenation was similar to the hydrogenation of rubber with an interacting functional group, such as the nitrile group in NBR. There are a number of reports showing that the hydrogenation activity of rhodium, ruthenium, osmium, and iridium complexes is inhibited by the coordination of a nitrile-functional group with the metal center.^{12,18,20,21}

Effect of the reaction temperature A series of experiments were carried out over the range of 120–140°C ([Ir] = 90 μ M, [C=C] = 246 mM, and P_{H_2} = 27.6 bar in monochlorobenzene) for CPIP hydrogenation and 130–150°C ([Ir] = 105 μ M, [C=C] = 152 mM, and P_{H_2} = 27.6 bar in monochlorobenzene) for NR hydrogenation. The effect of the temperature on the rate constant of hydrogenation for both rubbers can be represented by an Arrhenius plot, as shown in Figure 7. The linear plot indicates that a single rate-determining step is operative within the kinetic mechanism. The activation energy, calculated from least-squares regression analysis of $\ln k'$ versus the reciprocal of the temperature, was 79.8 kJ/mol for CPIP hydrogenation and 75.6 kJ/mol for NR hydrogenation. This provides further evidence that the kinetic data were obtained without a mass-transfer limitation and that the diffusion of the reactant was not a rate-determining factor under these conditions. Hydrogenation at a higher temperature exhibited a faster reaction rate and led to a higher efficiency. Although the hydrogenation rates of CPIP and NR catalyzed by OsHCl(CO)(O₂)(PCy₃)₂ were faster than that of the system in the presence of [Ir(COD)py(PCy₃)]PF₆, the apparent activation energy of the hydrogenation with the Ir catalyst was lower than that of the system catalyzed by the Os complex (109.3 kJ/mol for CPIP hydrogenation and 122.8 kJ/mol for NR hydrogenation). The hydrogenation catalyzed by the Ir catalyst was less sensitive to the reaction temperature than the Os system.

Effect of the solvent. The effects of different solvents on the hydrogenation rate of CPIP and NR in the presence of Crabtree's catalyst were investigated under base conditions: [Ir] = 90 μ M, P_{H_2} = 27.6 bar, and [C=C] = 246 mM at 130°C for CPIP hydrogenation and [Ir] = 105 μ M, P_{H_2} = 27.6 bar, and [C=C] = 152 mM at 140°C for NR hydrogenation. The results of these experiments are presented in Table VI. It shows that the chlorinated solvents chlorobenzene, dichloromethane, dichlorobenzene, and trichlorobenzene are viable solvents for the catalytic hydrogenation of CPIP hydrogenation with this cationic iridium catalyst, whereas the strong coordinating solvent tetrahydrofuran is not a good solvent for this Ir catalytic system, in contrast to Rh⁸ or Os^{19,22} catalysts. Crabtree⁸ studied alkene hydrogenation catalyzed by [Ir(COD)L₂]PF₆ and [Ir(COD)(py)L]PF₆ and found that noncoordinating solvents such as toluene, benzene, and hexane were inappropriate solvents because only catalytically inactive precipitates were formed under hydrogen. However, these Ir complexes were very active in noncoordinating solvents containing a chlorine atom, except for 1,1-dichloroethylene and carbon tetrachloride, because they failed to dissolve these Ir catalysts under a hydrogen atmosphere.⁹

TABLE VI
Effect of the Solvent on the Hydrogenation of CPIP and NR

Solvent	CPIP hydrogenation		NR hydrogenation	
	$k' \times 10^3$ (s ⁻¹)	Final hydrogenation (%)	$k' \times 10^3$ (s ⁻¹)	Final hydrogenation (%)
Chlorobenzene	1.92	98.1 (~35 min)	0.85	92.2 (~1 h)
Tetrahydrofuran	0.80	75.8 (~1 h)	—	—
Dichloromethane	2.16	96.6 (~30 min)	—	—
Dichlorobenzene	1.73	97.1 (~40 min)	0.74	93.8 (~1.5 h)
Trichlorobenzene	2.21	97.4 (~30 min)	0.59	85.8 (~1.2 h)

CPIP hydrogenation: [Ir] = 80 μ M, P_{H_2} = 27.6 bar, [C=C] = 246 mM, and temperature = 130°C. NR hydrogenation: [Ir] = 105 μ M, P_{H_2} = 27.6 bar, [C=C] = 152 mM, and temperature = 140°C.

Effect of the acid addition on the catalytic activity

Acid addition has been found to enhance the catalytic activity of olefinic hydrogenation catalysts. Guo and Rempel²³ reported that carboxylic acids increased the catalytic activity for the hydrogenation of an NBR emulsion catalyzed by RuCl(CO)(styryl)(PCy₃)₂. They suggested that the carboxylic acids were very effective in preventing the poisoning of the catalyst by impurities in the emulsion system. Yi et al.²⁴ also investigated the addition of acids with weakly coordinating anions such as trifluoromethanesulfonic acid and tetrafluoroboric acid/dimethyl ether complex (HBF₄ · OEt₂) which increased the rate of alkene hydrogenation with RuH(CO)(Cl)(PCy₃)₂. They surmised that the increase in the catalytic activity of this Ru catalytic species might be due to the selective entrapment of the phosphine ligand and the formation of a highly active 14-electron ruthenium-monophosphine phosphine species. In the case of NR hydrogenation, Charmondusit²⁵ and Hinchiranan et al.²² reported that the rate of NR hydrogenation in the presence of OsHCl(CO)-(O₂)(PCy₃)₂ could be increased by the addition of some acids such as 3-CPA and *p*-TSA. However, this behavior was disappointing for CPIP hydrogenation. Thus, it might be explained that the positive role of

acids in NR hydrogenation may be primarily due to the possible neutralization of impurities present in the rubber. In the system of NR hydrogenation catalyzed by [Ir(COD)py(PCy₃)]PF₆, the role of the acids, 3-CPA and *p*-TSA, in the hydrogenation of CPIP and NR were studied, and the results are presented in Tables VII and Figure 8.

The conversion profiles in Figure 8 indicate that the addition of 3-CPA and *p*-TSA enhanced the rate of NR hydrogenation. The results of 3-CPA for the Ir system were different from those for the Os system,²² in that the addition of 3-CPA exhibited a slower rate of hydrogenation catalyzed by the Os complex when monochlorobenzene was used as a solvent. To investigate the role of the acids in hydrogenation catalyzed by [Ir(COD)py(PCy₃)]PF₆, 3-CPA and *p*-TSA were also added to the CPIP solution. The acid addition could slightly increase the rate of CPIP hydrogenation. Therefore, it is possible to explain that the acid addition might promote the catalytic activity of [Ir(COD)py(PCy₃)]PF₆ by preventing the poisoning of the catalyst by proteins present in NR or other residual impurities from the polymerization process of CPIP. However, it cannot be concluded that the acid entrapped PCy₃ of the catalyst because Hu¹² reported

TABLE VII
Effect of Acid Addition on the Rate of Hydrogenation of CPIP and NR

Experiment	Rubber	Acid	[Acid] (mM)	[Acid]/[Ir]	Hydrogenation at 20 min (%)	$k' \times 10^3$ (s ⁻¹)
1	CPIP	—	—	—	81.9	1.48
2	CPIP	<i>p</i> -TSA	0.60	9.9	88.1	1.78
3	CPIP	3-CPA	0.63	10.6	89.3	1.85
4	NR	—	—	—	60.9	0.85
5	NR	<i>p</i> -TSA	0.53	5.0	74.2	1.37
6	NR	<i>p</i> -TSA	1.05	10.0	85.4	1.90
7	NR	<i>p</i> -TSA	2.11	20.1	86.4	2.10
8	NR	<i>p</i> -TSA	4.20	40.0	91.9	2.22
9	NR	3-CPA	0.56	5.3	79.6	1.56
10	NR	3-CPA	1.43	13.6	81.2	1.59
11	NR	3-CPA	2.22	21.1	81.8	1.57

CPIP hydrogenation: [Ir] = 60 μ M, P_{H_2} = 27.6 bar, [C=C] = 152 mM, and temperature = 130°C. NR hydrogenation: [Ir] = 105 μ M, P_{H_2} = 27.6 bar, [C=C] = 152 mM, and temperature = 140°C.

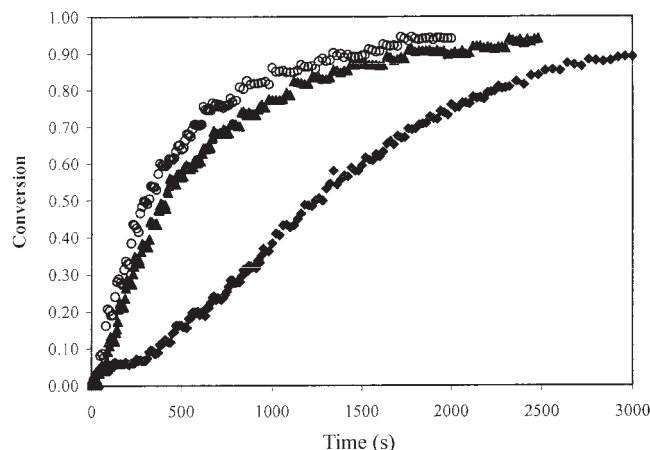
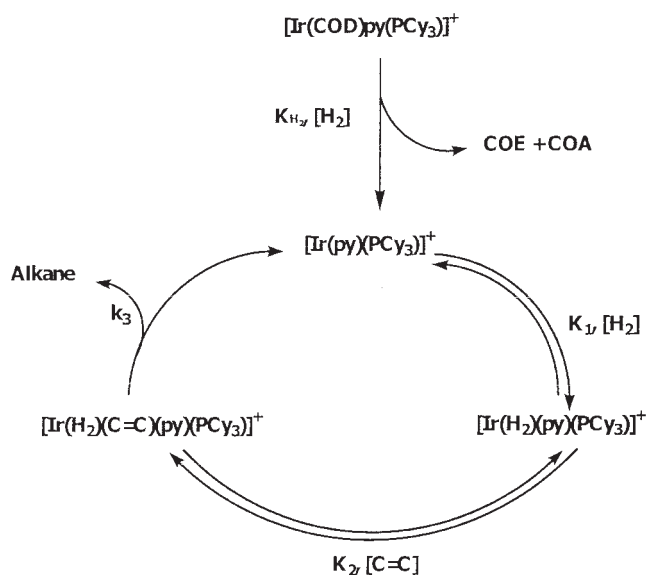


Figure 8 Comparison of NR hydrogenation conversion profiles for (◆) a nonacid addition system, (▲) the 21/1 [3-CPA]/[Ir] acid addition system, and (○) the 20/1 [p-TSA]/[Ir] acid addition system ([Ir] = 105 μM ; [C=C] = 152 mM; P_{H_2} = 27.6 bar; temperature = 140°C in monochlorobenzene).

that the peak of free PCy_3 dissociated from the catalyst precursor at 10 ppm was not present in the ^{31}P -NMR spectrum at 70°C; this indicated that no appreciable dissociation of the PCy_3 ligand occurred. However, carboxylic acids have been known to increase the catalytic activity of a catalyst in NR hydrogenation.^{22,25} An overload of these acids in the system might partially or totally deactivate Ir complexes, presumably by coordination.⁹

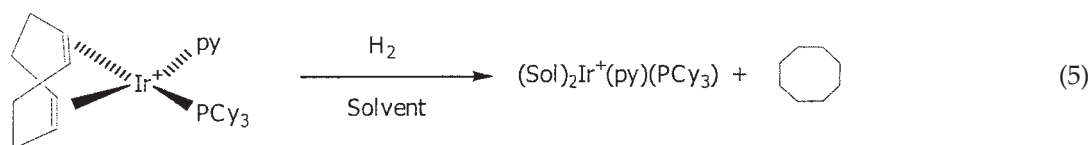
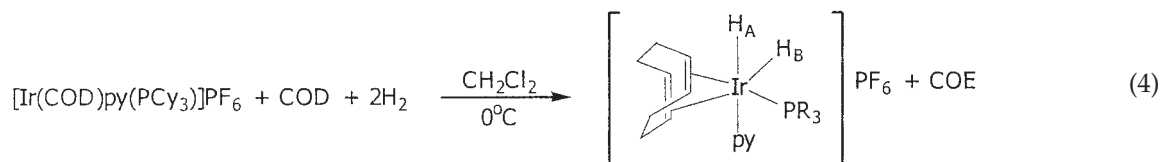
Reaction mechanism and rate law

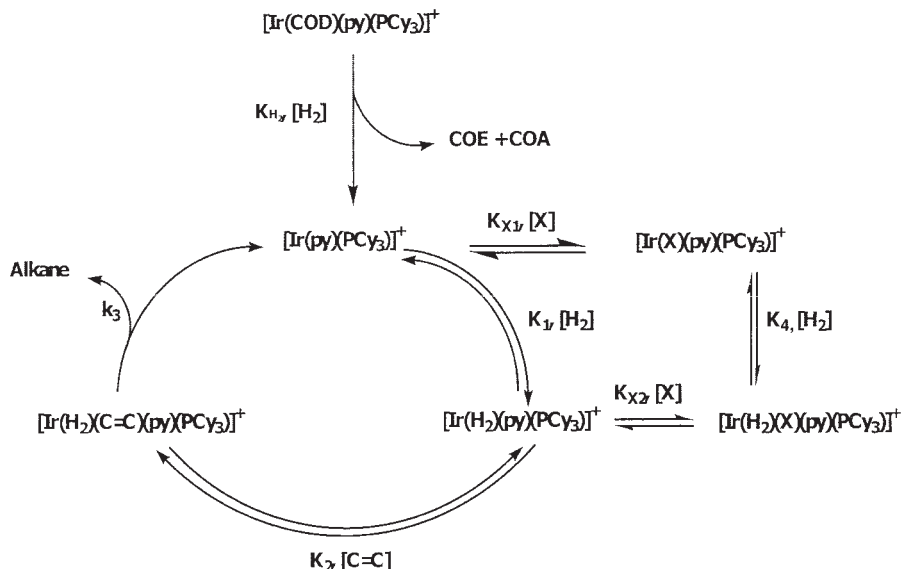
The catalytic pathway of olefinic hydrogenation in the presence of Crabtree's catalyst and its analogue has been investigated. The hydrogenation of diene polymers catalyzed by a homogeneous catalyst consists of many intermediate complexes. Thus, the manner in which to propose the catalytic mechanism of the hydrogenation of diene polymers is based on the inference of kinetic data and electron counting schemes. The catalytic cycle of $[\text{Ir}(\text{COD})-$



Scheme 1 Proposed mechanism for the hydrogenation of CPIP in the presence of $[\text{Ir}(\text{COD})\text{py}(\text{PCy}_3)]\text{PF}_6$.

$\text{py}(\text{PCy}_3)]\text{PF}_6$ in the hydrogenation of CPIP and NR is illustrated in Schemes 1 and 2, respectively. Crabtree²⁶ reported that $[\text{Ir}(\text{COD})\text{py}(\text{PR}_3)]\text{PF}_6$ ($\text{PR}_3 = \text{PCy}_3$ or $P\text{-}i\text{-Pr}_3$) reacts with H_2 at 0°C in CH_2Cl_2 in the presence of excess COD to produce *cis*-dihydro-diolefin complexes. Their stereochemistry is shown in eq. (4). Crabtree presented no evidence that $[\text{IrH}_2(\text{COD})\text{py}(\text{PR}_3)]\text{PF}_6$ could be formed via the direct activation of H_2 by $[\text{Ir}(\text{COD})\text{py}(\text{PR}_3)]\text{PF}_6$ in the absence of excess (COD) because pyridine, a donor ligand, inhibited H_2 addition to $[\text{Ir}(\text{COD})\text{py}(\text{PCy}_3)]\text{PF}_6$, which was different from other donor ligands that favored H_2 addition to the metal center. However, the active catalyst could be formed in the presence of H_2 and a noncoordinating solvent, presumably via the reduction of COD to cyclooctene (COE) or cyclooctane, as shown in eq. (5). It is particularly effective for the reduction of highly substituted alkenes because the $[\text{Ir}(\text{py})(\text{PCy}_3)]^+$ fragment is not very bulky:^{27,28}





Scheme 2 Proposed mechanism for the hydrogenation of NR in the presence of $[\text{Ir}(\text{COD})\text{py}(\text{PCy}_3)]\text{PF}_6$.

where R is Cy or *P-i-Pr*. This 12-electron active species, $[\text{Ir}(\text{py})(\text{PCy}_3)]^+$, reacts with the H_2 molecule to generate the dihydrido iridium complex, $[\text{Ir}(\text{H}_2)(\text{py})(\text{PCy}_3)]^+$. The substrate double bond coordinates to the dihydrido catalyst. Then, the hydrogen is transferred to the π -olefin complex to obtain an alkyl complex. The alkyl complex is cleaved by a transferred hydride to form the hydrogenated polymer and to regenerate the cationic active species.

According to the proposed mechanism, the hydrogenation of CPIP and NR by iridium is provided by the following rate expression:

$$-\frac{d[\text{C}=\text{C}]}{dt} = k_3[\text{Ir}(\text{H}_2)(\text{C}=\text{C})(\text{py})(\text{PCy}_3)]^+ \quad (6)$$

A material balance on the active species of iridium charged to the hydrogenation system of CPIP is given as follows:

$$[\text{Ir}]_T = [\text{Ir}(\text{H}_2)(\text{C}=\text{C})(\text{py})(\text{PCy}_3)]^+ + [\text{Ir}(\text{H}_2)(\text{py})(\text{PCy}_3)]^+ + [\text{Ir}(\text{py})(\text{PCy}_3)]^+ \quad (7)$$

The effect of impurities (X) in NR on the hydrogenation rate can be compared to the effect of the nitrile-functional group, which inhibits the catalytic activity in NBR hydrogenation.¹² It is possible that impurities in NR might coordinate with unsaturated active species of a catalyst to reduce the hydrogenation activity, as shown in Scheme 2. A material balance on the active species of the Ir catalyst for the NR hydrogenation can be expressed as follows:

$$[\text{Ir}]_T = [\text{Ir}(\text{H}_2)(\text{C}=\text{C})(\text{py})(\text{PCy}_3)]^+ + [\text{Ir}(\text{H}_2)(\text{py})(\text{PCy}_3)]^+ + [\text{Ir}(\text{py})(\text{PCy}_3)]^+ + [\text{Ir}(\text{X})(\text{py})(\text{PCy}_3)]^+ + [\text{Ir}(\text{H}_2)(\text{X})(\text{py})(\text{PCy}_3)]^+ \quad (8)$$

Every iridium complex species concentration term in eqs. (7) and (8) can be expressed in terms of $[\text{Ir}(\text{H}_2)(\text{C}=\text{C})(\text{py})(\text{PCy}_3)]^+$ with the equilibria defined in Scheme 1 and Scheme 2 and then can be substituted into eq. (6) to provide the resulting rate law, as shown in eq. (9) for CPIP hydrogenation and in eq. (10) for NR hydrogenation:

$$-\frac{d[\text{C}=\text{C}]}{dt} = \frac{k_3 K_1 K_2 [\text{Ir}]_T [\text{C}=\text{C}] [\text{H}_2]}{1 + K_1 [\text{H}_2] (1 + K_2 [\text{C}=\text{C}])} \quad (9)$$

$$-\frac{d[\text{C}=\text{C}]}{dt} = \frac{k_3 K_1 K_2 [\text{Ir}]_T [\text{C}=\text{C}] [\text{H}_2]}{1 + K_{X1} [\text{X}] + K_1 [\text{H}_2] (1 + K_2 [\text{C}=\text{C}] + K_{X2} [\text{X}])} \quad (10)$$

Although the rate expression would suggest that there would be a zero-order dependence on $[\text{H}_2]$, the kinetic observations indicated that the hydrogenation rate was first-order with respect to P_{H_2} . It can be presumed that K_1 , K_2 , and K_{X2} were very small for the range of the reaction conditions and substrate concentrations used in this study. The reaction exhibited a first-order response of k' to $[\text{Ir}]$ at a low concentration of the catalyst and a shift to a zero-order dependence at a higher concentration of the catalyst because of the possible dimerization of the catalyst. For NR hydrogenation, the effect of impurities in NR is an important factor in reducing the rate of hydrogenation. The rate expression, eq. (10), shows that the rate of NR hydrogenation decreased with increasing rubber concentra-

tion, and this is in line with an increase in the amount of impurities.

Relative viscosity (η_{rel}) of HCPIP and HNR

One of the major problems associated with the modification of polymers is side reactions such as chain degradation and crosslinking, which often accompany the desirable modification reaction. These side reactions indicate a change in the chain length properties of the parent macromolecules during the chemical modification process. Although FTIR or $^1\text{H-NMR}$ spectroscopy is the usual technique to evaluate the degree of hydrogenation, these methods are not sufficient to detect the side reactions, crosslinks and degradation, that cause the undesirable properties. Therefore, the degree of polymer crosslinking must be inferred indirectly from molecular weight measurements. The dilute solution viscosity, related to the morphology and microstructure of polymer chains, has been used to monitor the shifts in the molecular weight that are created by crosslinking or degradation. The viscosity of dilute CPIP and NR solutions before and after the hydrogenation process with respect to a pure solvent (η_{rel}) provides a simple and effective means of measuring the consequences of the crosslinking and degradation of samples.

The effects of the catalyst concentration, polymer concentration, and P_{H_2} on η_{rel} of CPIP and NR after the hydrogenation process, compared with an inherent viscosity, are shown in Figure 9. Over the range of conditions investigated (for CPIP, $\eta_{rel} = 4.48$, $[\text{Ir}] = 30\text{--}150\ \mu\text{M}$, $[\text{C}=\text{C}] = 163\text{--}500\ \text{mM}$, and $P_{\text{H}_2} = 13.8\text{--}52.2\ \text{bar}$ at 130°C ; for NR, $\eta_{rel} = 7.32$, $[\text{Ir}] = 65\text{--}145\ \mu\text{M}$, $[\text{C}=\text{C}] = 100\text{--}260\ \text{mM}$, and $P_{\text{H}_2} = 13.8\text{--}55.1\ \text{bar}$ at 140°C), the η_{rel} values of both hydrogenated rubbers are higher than those of CPIP and NR. The increase in η_{rel} suggests that no degradation occurred during the catalytic hydrogenation reaction. Because η_{rel} of HCPIP remained constant, it can be concluded that a very small amount of residual $\text{C}=\text{C}$ remained after the hydrogenation reaction and also that crosslinking possibly did not affect the hydrogenation process.^{19,29}

For NR hydrogenation, Figure 9 shows that the viscosity of HNR, varied over the range of 7.03–9.81, was dependent on the reaction conditions, the degree of hydrogenation, and the reaction time. η_{rel} of the HNR samples was higher when the samples were hydrogenated at a high catalyst loading or a low rubber concentration. Similar results were observed for NBR hydrogenation catalyzed by this Ir complex.¹² As for the effect of P_{H_2} , η_{rel} of HNR increased with P_{H_2} . The reason for this phenomenon is not obvious; however, it is possible that higher P_{H_2} might promote gel formation for this hydrogenation system.

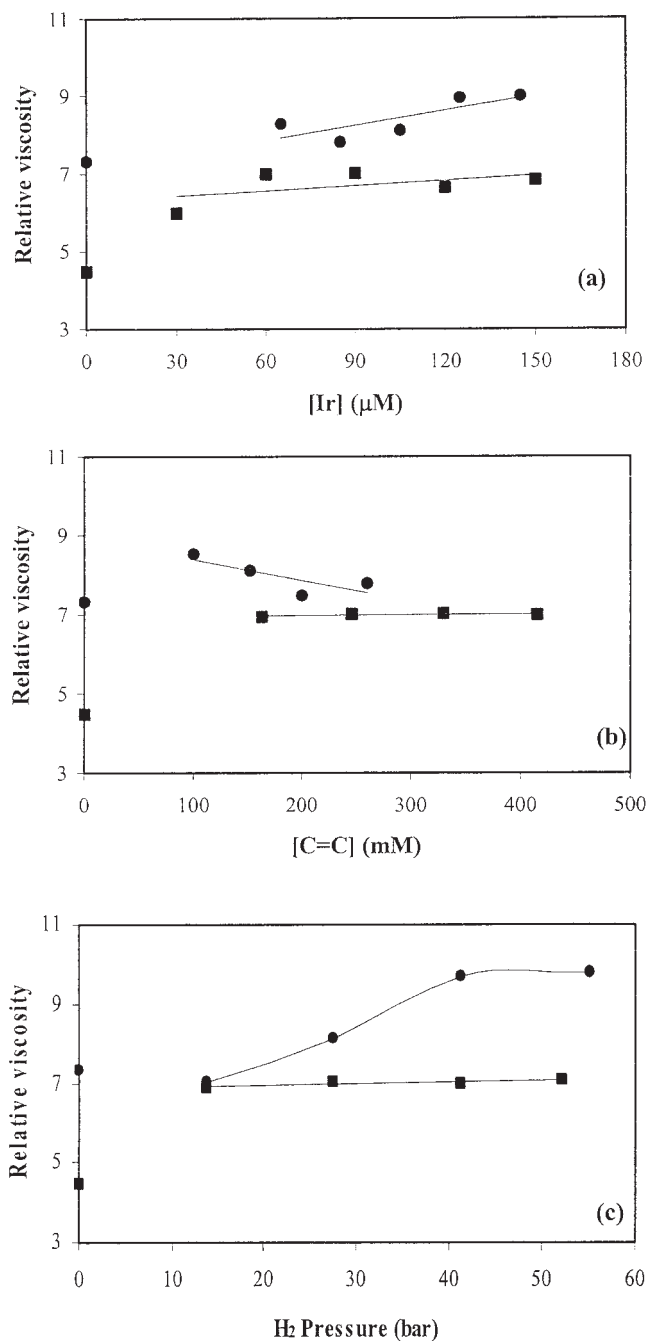


Figure 9 Comparison of the η_{rel} values for (■) CPIP and (●) NR after hydrogenation: (a) η_{rel} as a function of the total metal loading for CPIP hydrogenation ($P_{\text{H}_2} = 27.6\ \text{bar}$; $[\text{C}=\text{C}] = 246\ \text{mM}$; temperature = 130°C) and NR hydrogenation ($P_{\text{H}_2} = 27.6\ \text{bar}$; $[\text{C}=\text{C}] = 152\ \text{mM}$; temperature = 140°C), (b) η_{rel} as a function of the polymer loading for CPIP hydrogenation ($[\text{Ir}] = 90\ \mu\text{M}$; $P_{\text{H}_2} = 27.6\ \text{bar}$; temperature = 130°C) and NR hydrogenation ($[\text{Ir}] = 105\ \mu\text{M}$; $P_{\text{H}_2} = 27.6\ \text{bar}$; temperature = 140°C), and (c) influence of P_{H_2} on η_{rel} for CPIP hydrogenation ($[\text{Ir}] = 90\ \mu\text{M}$; $[\text{C}=\text{C}] = 246\ \text{mM}$; temperature = 130°C) and NR hydrogenation ($[\text{Ir}] = 105\ \mu\text{M}$; $[\text{C}=\text{C}] = 152\ \text{mM}$; temperature = 140°C).

TABLE VIII
Degradation Temperatures and T_g Values
of the Rubber Samples

Rubber sample	T_g (°C)	T_{id} (°C)	T_{max} (°C)
CPIP	-55.5	346.2	367.0
HCPIPOs	-52.2	427.1	448.0
HCPIPIr	-52.6	420.0	440.0
NR	-62.3	357.2	380.9
HNROs	-60.5	433.5	462.1
HNRIr	-60.9	430.7	459.7
EPDM ^a	-44.6	452.7	470.7

^a EPDM had an ethylene/propylene ratio of 50/50 and a diene concentration of 9.5%.

Thermal properties of HCPIP and HNR

TGA of CPIP, NR, and their hydrogenated products with OsHCl(CO)(O₂)(PCy₃)₂ (for HCPIPOs, [Os] = 70 μM, P_{H_2} = 20.7 bar, [C=C] = 260 mM, and temperature = 130°C; for HNROs, [Os] = 100 μM, P_{H_2} = 27.6 bar, [C=C] = 260 mM, and temperature = 140°C) and [Ir(COD)py(PCy₃)]PF₆ (for HCPIPIr, [Ir] = 90 μM, P_{H_2} = 27.6 bar, [C=C] = 246 mM, and temperature = 130°C; for HNRIr, [Ir] = 105 μM, P_{H_2} = 27.6 bar, [C=C] = 152 mM, and temperature = 140°C), and EPDM were conducted under a nitrogen atmosphere. Table VIII summarizes T_{id} and T_{max} of all rubber samples. The degradation temperature (T_{id} and T_{max}) of HCPIP and HNR catalyzed by both catalysts were higher than those of CPIP and NR. The results suggest that the degradation temperature increased with increasing reduction of carbon-carbon double bonds in CPIP and NR. This can be explained, in that the C=C bonds in both rubbers consist of a strong σ bond and a weak π bond and the hydrogenation reaction involves the breakage of a weak π bond by the hydrogen molecule to form a stronger C-H σ bond, which leads to higher thermal stability. In comparison with those of standard EPDM rubber, the degradation temperatures of HCPIP and HNR were very close to those of EPDM rubber. It can be concluded that HCPIP and HNR provide a facile entry to alternating EPDMs.^{30,31}

DSC was used to determine T_g of hydrogenated rubber. T_g is the temperature at which the amorphous domains of a polymer take on the characteristic properties of the glassy state: brittleness, stiffness, and rigidity. This was determined from the midpoint of the baseline shift of the DSC thermogram. T_g obtained from the DSC thermogram is presented in Table VIII. The T_g values of CPIP and NR, -55.5 and -62.3°C, respectively, demonstrate the rubber properties at room temperature and the glass properties below T_g . The standard EPDM rubber, having the higher T_g value of -44.6°C, exhibits a higher degree of crystallization in the polymer structure than that of CPIP and NR. The T_g values of HCPIP and HNR were slightly higher than those of their parent materials. Thus, it can

be concluded that the hydrogenation reaction does not appreciably affect T_g of CPIP and NR. Consequently, the hydrogenated rubber products still have very amorphous properties. This agrees very well with the results obtained for NR hydrogenation with RhCl(PPh₃)₃, which had no effect on T_g of the HNR product.³²

CONCLUSIONS

In monochlorobenzene, [Ir(COD)py(PCy₃)]PF₆ was an efficient catalyst precursor for the hydrogenation of CPIP and NR. The hydrogenation of both rubbers exhibited a first-order dependence on P_{H_2} and a first-to-zero-order dependence with respect to the catalyst concentration. The reaction kinetics implied that the active complex was a mononuclear species at a low catalyst concentration and that a side reaction such as dimerization of the Ir catalyst might have occurred at a higher catalyst loading. Impurities in NR caused the hydrogenation rate to exhibit an inverse behavior with respect to the rubber concentration, whereas the rate of CPIP hydrogenation remained constant when the loading of rubber was increased. The apparent activation energy for the hydrogenation of CPIP and NR was found to be 79.8 and 75.6 kJ/mol, respectively. The proposed mechanism and the rate expression for hydrogenation of both CPIP and NR in the presence of [Ir(COD)py(PCy₃)]PF₆ were consistent with the kinetic data. η_{rel} of the hydrogenated products indicated that there was probably no degradation for either hydrogenated rubber. However, crosslinking might have occurred at high P_{H_2} values in NR hydrogenation. The increase in the degradation temperature of the hydrogenated rubber products demonstrates that hydrogenation increases the thermal stability of CPIP and NR without affecting T_g .

Gratitude to Neil T. McManus for technical assistance is acknowledged.

References

1. Morton, M. *Rubber Technology*; Van Nostrand Reinhold: New York, 1973; p 152.
2. Tanaka, Y. *Rubber Chem Technol* 2001, 74, 355.
3. McManus, N. T.; Rempel, G. L. *Rev Macromol Chem Phys* 1995, 35, 239.
4. Nang, T. D.; Katabe, Y.; Minoura, Y. *Polymer* 1976, 17, 117.
5. Chang, J. R.; Huang, S. M. *Ind Eng Chem Res* 1998, 37, 1220.
6. Cassano, S. A.; Valles, E. M.; Quinzani, L. M. *Polymer* 1998, 39, 5573.
7. Bhaduri, S.; Mukesh, D. *Homogeneous Catalysis Mechanisms and Industrial Applications*; Wiley: New York, 2000.
8. Crabtree, R. H. *Acc Chem Res* 1979, 12, 331.
9. Crabtree, R. H.; Felkin, H.; Morris, G. E. *J Organomet Chem* 1977, 141, 205.
10. Gilliom, L. R. *Macromolecules* 1989, 22, 662.
11. Gilliom, L. R.; Honnell, K. G. *Macromolecules* 1992, 25, 6066.

12. Hu, J. Master's Thesis, University of Waterloo, 2000.
13. Stork, G.; Kahne, D. E. *J Am Chem Soc* 1983, 105, 1072.
14. Mohammadi, N. A.; Rempel, G. L. *Comput Chem Eng* 1987, 11, 27.
15. Aik-Hwee, E.; Tanaka, Y.; Seng-Neon, G. *J Nat Rubber Res* 1992, 7, 152.
16. Mason, R. L.; Gunst, R. F.; Hess, L. H. *Statistical Design and Analysis of Experiments*; Wiley: New York, 1989.
17. Crabtree, R. H.; Davis, M. W. *J Org Chem* 1986, 51, 2655.
18. Parent, J. S.; McManus, N. T.; Rempel, G. L. *Ind Eng Chem Res* 1996, 35, 4417.
19. Charmondusit, K.; Pasassarakich, P.; McManus, N. T.; Rempel, G. L. *J Appl Polym Sci* 2003, 89, 142.
20. Parent, J. S.; McManus, N. T.; Rempel, G. L. *Ind Eng Chem Res* 1998, 37, 4253.
21. Martin, P.; McManus, N. T.; Rempel, G. L. *J Mol Catal A* 1997, 126, 115.
22. Hinchiranan, N.; Prasassarakich, P.; Rempel, G. L. *J Appl Polym Sci*, to appear.
23. Guo, X. Y.; Rempel, G. L. *J Appl Polym Sci* 1997, 65, 667.
24. Yi, C. S.; Lee, D. W.; He, Z. *Organometallics* 2000, 19, 2909.
25. Charmondusit, K. Ph.D. Thesis, Chulalongkorn University, 2002.
26. Crabtree, R. H.; Felkin, H.; Fillbeen-Khan, T.; Morris, G. E. *J Organomet Chem* 1979, 168, 183.
27. Dickson, R. S. *Homogeneous Catalysis with Compounds of Rhodium and Iridium*; Wiley: New York, 1985; p 67.
28. Crabtree, R. H. *The Organometallic Chemistry of the Transition Metals*; Wiley: New York, 2001; p 230.
29. Parent, J.; McManus, N. T.; Rempel, G. L. *J Appl Polym Sci* 2001, 79, 1618.
30. Hoffmann, W. *Rubber Technology Handbook*; Hanser: Munich, 1989; p 85.
31. Ginic-Markovic, M.; Roy Choudhury, N.; Dimopoulos, M.; Williams, D. R. G.; Matison, J. *Thermochim Acta* 1998, 316, 87.
32. Singha, N. K.; De, P. P.; Sivaram, S. *J Appl Polym Sci* 1997, 66, 1647.